

## Research Article

# Design and Experimental Validation of a Portable Photometer for Non-Invasive Neonatal Jaundice Assessment

M. J. Dinparvar <sup>a</sup> and M. Khanlari <sup>\*b</sup>

*a* Department of Biomedical Engineering, NT.C., Islamic Azad University, Tehran, Iran

*b* Department of Biomedical Engineering, NT.C., Islamic Azad University, Tehran, Iran

**\*Corresponding Author Email: [msmkhanlari@iau.ac.ir](mailto:msmkhanlari@iau.ac.ir)**

DOI: 10.71498/ijbbe.2025.1211116

## ABSTRACT

Received: Jul. 5, 2025, Revised: Aug. 5, 2025, Accepted: Aug. 16, 2025, Available Online: Sep. 4, 2025

*Background and Objective:* Bilirubin, a yellow pigment, is a key biomarker for diagnosing and monitoring neonatal jaundice. Neonatal jaundice, caused by elevated blood bilirubin levels, can lead to severe complications if not detected and treated in time. Traditional methods for bilirubin measurement, although accurate, are invasive and require laboratory equipment, causing discomfort for the infant and increasing costs. This study presents the design and evaluation of a portable photometer for accurate non-invasive bilirubin measurement.

### Methods:

The proposed device utilizes blue light at a wavelength of 470 nm to determine bilirubin concentration based on reflected light from simulated skin surfaces. The system incorporates multiple optical filters and advanced calibration algorithms to minimize errors caused by environmental and physical factors such as ambient light, temperature, and skin tone variations.

### Results:

Experimental tests on skin phantoms with various bilirubin concentrations demonstrated the device's high accuracy in measuring bilirubin across a range of conditions, including light, medium, and dark skin tones.

### Conclusion:

The results indicate that portable photometers can serve as rapid, accurate, and user-friendly tools in clinical and medical settings, particularly in environments with limited access to laboratory facilities.

## KEYWORDS

Neonates Jaundice, Photometry, Transcutaneous Bilirubin

## I. INTRODUCTION

Bilirubin is a yellow pigment generated during the breakdown of hemoglobin. Elevated levels of this pigment in the blood lead to jaundice, a common physiological condition particularly prevalent in newborns [1, 2]. It is observed in approximately 60% of full-term and up to 80% of preterm neonates and is primarily due to accelerated hemoglobin turnover and the temporary immaturity of the liver's bilirubin clearance mechanism. If not diagnosed and treated promptly, neonatal jaundice may result in irreversible neurological complications [3].

The conventional method for diagnosing jaundice is based on measuring the total serum bilirubin (TSB) through blood sampling. Although this method provides high accuracy, it is invasive and may cause discomfort or even anemia in newborns [4, 5]. Furthermore, it requires laboratory equipment and is both time-consuming and expensive. As a result, non-invasive techniques such as transcutaneous bilirubinometry (TcB) have been developed in

recent years as effective alternatives to blood-based methods [6, 7].

Photometry is one such non-invasive method for estimating bilirubin concentration based on its selective absorption of light at specific wavelengths, particularly in the blue spectrum.

Photometric devices illuminate the skin and analyze the reflected light using calibration algorithms to estimate bilirubin concentration [8–10]. Bilirubin exhibits a distinct absorption peak in the 450–490 nm range [11, 12], which enables the design of simple and cost-effective optical diagnostic tools. Fig. 1 illustrates the absorption spectra of various tissue components, including hemoglobin, melanin, water, and bilirubin [13, 19].

In this study, a portable photometric device was designed and evaluated to provide a simple, rapid, and cost-effective solution for the initial screening of neonatal jaundice. This research is categorized as applied and is intended for use in clinical settings with limited access to laboratory infrastructure.

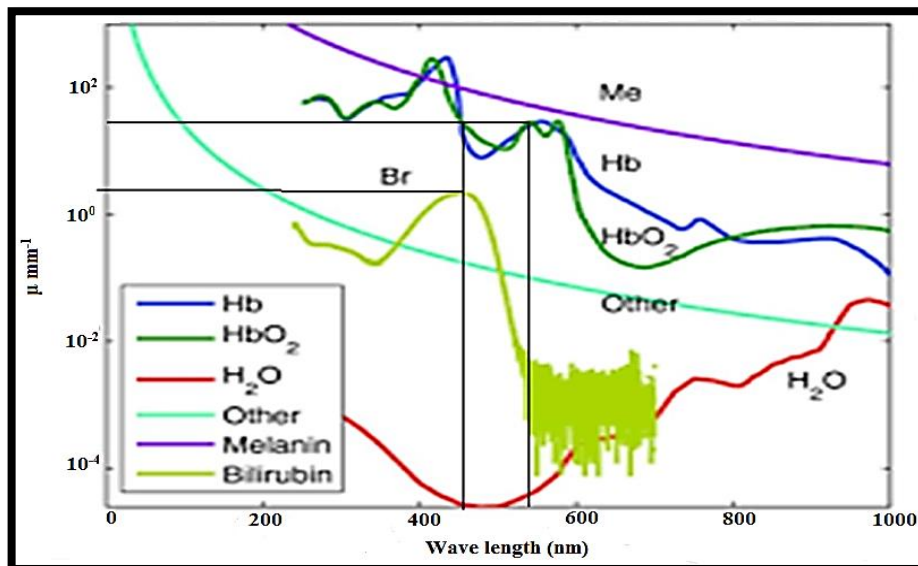


Fig. 1 Representative Absorption Spectra of Blood Constituents [13, 19]

Transcutaneous bilirubin measurement has emerged as a simple and non-invasive alternative to traditional invasive methods. By

eliminating the need for blood sampling, it enables early screening and facilitates timely diagnosis and treatment.[10]

In recent years, numerous studies have focused on the development and enhancement of photometric devices for neonatal jaundice detection. These devices leverage modern optical technologies to deliver reliable and consistent non-invasive bilirubin measurements [11–14]. Techniques such as diffuse reflectance spectroscopy (DRS) analyze light reflected from the skin to estimate bilirubin concentration, even in turbid samples [11]. Furthermore, photon diffusion theory-based models have improved the accuracy of TcB methods by simulating light propagation in neonatal skin.[12]

The design of portable, handheld systems capable of simultaneously measuring bilirubin and hemoglobin represents a major step toward the clinical translation of such technologies. These devices enhance accessibility and enable rapid monitoring in both hospital and home settings.[13]

Comparative studies between TcB and the gold standard TSB have shown that optical methods exhibit acceptable accuracy and strong correlation with serum values, making them reliable tools for initial screening and treatment monitoring [14]. Moreover, computational and machine learning models have been employed to analyze neonatal data for the prediction of jaundice severity and therapy planning.[16,15]

Various phototherapy systems have also been developed using different illumination techniques, including photometry and spectrophotometry, to reduce serum bilirubin levels in affected neonates [17]. These innovations highlight the increasing potential of optical technologies in both diagnosis and treatment.

Given the limitations of traditional methods and the advantages of photometric approaches, developing portable and efficient devices for transcutaneous bilirubin estimation is a promising direction in neonatal care. In this study, we present the design and evaluation of a portable photometric device aimed at providing an accurate, rapid, and user-friendly

solution for neonatal jaundice screening and follow-up.

## II. MATERIALS AND METHODS

### A. Preparation of Skin-Mimicking Phantoms

To evaluate the accuracy of the bilirubin measurement device under laboratory-simulated conditions, gelatin-based optical phantoms were fabricated to mimic the optical properties of human skin. These phantoms replicate light absorption and scattering behavior in tissue, allowing controlled assessment of the device's response to various bilirubin concentrations. The phantom fabrication method was adapted based on previous studies on optical simulation of neonatal skin [11, 13]. To simulate bilirubin absorption, food-grade dyes with a similar spectral profile were used. This approach offers cost-effectiveness, reproducibility, and standardization across measurements. The phantoms were prepared in three categories:

#### (a) Control Samples:

To produce phantoms with controlled bilirubin concentrations, a 2% (w/v) gelatin solution was prepared by gradually dissolving gelatin powder into deionized water. The mixture was heated to 60°C and stirred using a magnetic stirrer to ensure homogeneity. Standard dye solutions with concentrations of 0.25, 0.3, and 0.5 mg/dL were prepared by adding 5, 7, and 10  $\mu$ L of dye, respectively, to the gelatin base. After thorough mixing, the solutions were poured into sterile containers and allowed to solidify at room temperature.

#### (b) High-Concentration Samples:

To assess device performance at higher bilirubin levels, more concentrated dye solutions were used. Volumes of 100, 150, and 200  $\mu$ L of concentrated dye were added to 2% gelatin to achieve final concentrations of 2, 3, and 4 mg/dL, respectively. The mixtures were

homogenized using a magnetic stirrer, poured into transparent molds, and left to set at room temperature for two hours until gel formation occurred (Fig. 2).

### (c) Dark Skin Model Samples

To simulate the optical properties of dark skin tones more accurately, a coffee solution was used as a background light absorber. A solution with a concentration of 250 mg/dL was prepared and added to the gelatin mixture as a melanin-mimicking agent. Food-grade dye solutions with varying concentrations (as described in previous sections) were added to the coffee-infused phantoms.

To ensure uniform distribution of both the dye and the coffee particles, the mixtures were treated in an ultrasonic bath for 5 minutes. The final solutions were poured into sterile molds and allowed to solidify at room temperature, forming stable gel-based phantoms (Fig. 3).

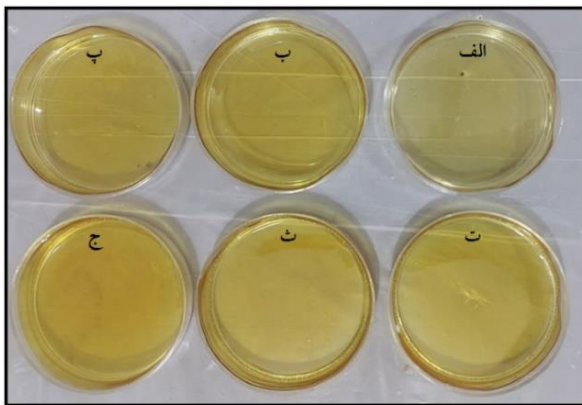


Fig. 2 Phantoms with Different Bilirubin Concentrations. (a) 0.25, (b) 0.3, (c) 0.5, (d) 2, (e) 3, and (f) 4 mg/dL

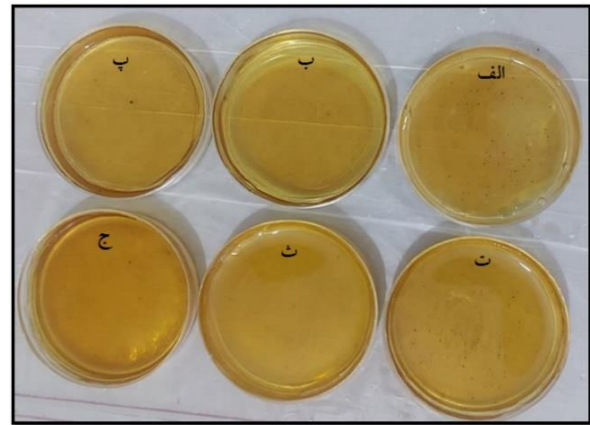


Fig. 3 Coffee-Infused Phantoms with Varying Bilirubin Concentrations. (a) 0.25, (b) 0.3, (c) 0.5, (d) 2, (e) 3, and (f) 4 mg/dL

### B. System Design

In the proposed device, a constant current power supply was used to drive the LEDs, minimizing intensity fluctuations and ensuring stable illumination. The light emitted from the LEDs is focused using a set of precision lenses and directed onto the surface of the skin or phantom. The optical system is carefully designed to optimize beam direction and intensity while minimizing optical losses.

The lenses used are coated with anti-reflective material to enhance transmission efficiency. The emitted blue light interacts with bilirubin molecules within the skin tissue, and part of it is absorbed. The reflected or transmitted portion of the light is collected and directed toward an optical sensor.

This reflected signal contains spectral information about bilirubin concentration in the superficial skin layers, which is then analyzed by the system for estimation and display.

To ensure accurate measurement of reflected light intensity, a TSL2561 digital light sensor was employed. This sensor offers significant noise reduction as light intensity increases and provides a digital output directly to the microcontroller, eliminating the need for analog-to-digital conversion. To minimize external influences—such as light angle, device-to-skin distance, and applied pressure—a mechanical enclosure was designed with



precise dimensions. A fixed distance of 1.25 cm between the sensor and the skin surface was maintained to ensure measurement consistency. Additionally, the device was fitted with a light-blocking shield to prevent interference from ambient illumination. Fig. 4 illustrates the precise mechanical design used to maintain a fixed distance between the sensor and the skin. This structure helps reduce measurement errors caused by variations in light angle and distance.

The electronic control unit is based on an Arduino Mega 2560 board utilizing an ATmega2560 microcontroller from AVR. This board supports both I2C and SPI communication protocols. The I2C protocol was used to interface with the light sensor, while SPI was utilized for communication with the display module.

The microcontroller processes the incoming digital signals, applies noise filtering algorithms, and computes the estimated bilirubin concentration. To enhance accuracy, multiple consecutive readings under identical conditions were taken, and the average signal was calculated. The device was calibrated using standard bilirubin solutions at various concentrations, simulating real clinical levels. The processed results are displayed numerically on the device screen.

To facilitate portability and usability in clinical environments, the system is powered by a rechargeable lithium battery, which supports approximately 1,800 tests per full charge.



Fig. 4 Custom-Designed Mechanical Fixture for Sensor and LED Placement

### III. DISCUSSION

The engineering design of the device aimed to deliver a compact, reliable, and clinically viable solution, with final dimensions of  $12 \times 8$  cm and a weight of 800 grams. Fig. 5 shows the final physical configuration of the fabricated device. During the design process, several critical factors were considered, including ease of use, portability, reliability across various ambient lighting and temperature conditions, and mechanical robustness. Ultimately, an optimized structural configuration was proposed to meet clinical and operational needs for use in real-world medical environments.



Fig. 5 Physical Structure of the Device

#### A. Bilirubin Estimation

To estimate bilirubin concentration in tissue, the Beer-Lambert law was applied—an essential principle in spectrophotometry that

describes the linear relationship between light absorbance, the concentration of an absorbing substance, and the optical path length.

This relationship is mathematically expressed as Eq. 1.

$$I(\lambda) = I_0(\lambda)F \cdot 10^{-K} \quad (1)$$

where  $I_0(\lambda)$  is the intensity of the incident light at the wavelength  $\lambda$ ,  $I(\lambda)$  is the reflected light intensity measured by the sensor,  $K$  is the absorption coefficient and  $F$  is the attenuation factor that reflects light absorption and scattering within the tissue and depends on bilirubin concentration [19].

Equation 2 relates the absorption coefficient to the concentration of the absorbing substance ( $C$ ), its molar absorptivity ( $\epsilon$ ), and the optical path length through the tissue ( $L$ ). This fundamental relationship forms the basis for spectroscopic analysis in biological tissues.

$$K = \epsilon CL \quad (2)$$

In this study, reflectance measurements were taken at three different wavelengths to enhance estimation accuracy. Multi-wavelength analysis allows compensation for spectral interference caused by other chromophores present in the skin, such as hemoglobin and melanin, thereby improving specificity for bilirubin detection.

According to Fig. 1, oxyhemoglobin and bilirubin exhibit similar absorption behavior at a wavelength of 470 nm (blue light). However, bilirubin absorbs significantly less light at 530 nm (green light). By measuring light absorbance at both wavelengths and calculating their difference, the influence of oxyhemoglobin can be minimized, allowing for a more accurate estimation of bilirubin concentration [9].

Another major factor affecting light absorption at 470 nm is melanin, the primary skin pigment. Melanin exhibits relatively uniform absorption across a broad spectrum of wavelengths, particularly between 450 and 700 nm. To reduce melanin's effect on bilirubin measurement, absorption at 450 nm and 630 nm (red light) can be analyzed and computationally corrected.

As a result, utilizing three distinct wavelengths enables the attenuation of interference from both hemoglobin and melanin, thereby enhancing measurement accuracy and specificity.

In this study, the above principles were applied to analyze reflectance data from skin-mimicking phantoms at multiple wavelengths. Bilirubin concentrations were calculated using this approach, which yielded improved precision and repeatability compared to traditional single-wavelength methods. The proposed technique demonstrates potential as a reliable and non-invasive method for bilirubin quantification in biological tissues.

## **B. Phantoms with Varying Bilirubin Concentrations**

In both phantom groups (with and without coffee), bilirubin concentration was adjusted at six different levels: 0.25, 0.3, 0.5, 2, 3, and 4 mg/dL. This concentration range was selected to cover clinically relevant values and to evaluate the device's accuracy across different bilirubin levels.

For each phantom sample, reflectance measurements were taken at three distinct surface locations, and three consecutive readings were recorded per location. As a result, a total of 9 reflectance values were obtained for each bilirubin concentration, providing sufficient data for statistical analysis (Fig. 6).

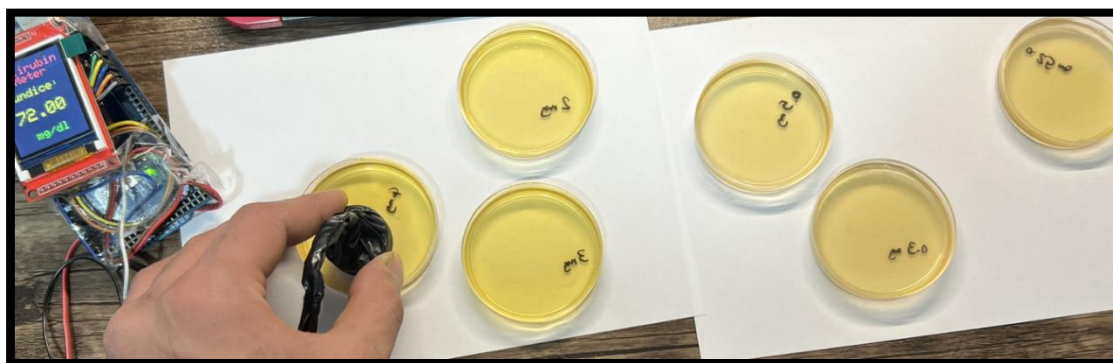


Fig. 6 Device Testing on Phantom Samples

Following data acquisition, the reflectance spectra for each sample were linearly matched against standard reference spectra of chromophores present in the phantom composition (including food dye, coffee, gelatin, and water). This spectral fitting enabled the identification of absorption contributions from each component. Subsequently, the Beer–Lambert law was applied to estimate the concentration of each chromophore, yielding high accuracy in bilirubin quantification.

The detailed measurement results are presented in Tables 1 and 2. In these Tables, “Error” shows the signed difference ( $\pm$ ) between measured and actual values, and “Absolute Error (%)” is the absolute percentage error.

The Pearson correlation coefficient ( $r$ ), which quantifies the strength and direction of a linear relationship between two variables, was calculated as 0.9997 and 0.9976 for Tables 1 and 2, respectively. These values, being very close to +1, indicate a very strong positive correlation between the actual and estimated bilirubin concentrations.

In other words, as the actual bilirubin concentration increases, the estimated concentration also increases in a nearly linear manner. This result confirms the high accuracy and reliability of the proposed method for bilirubin quantification in this study (Figs. 7 and 8).

Table 1: Reflected Light Intensity at Different Bilirubin Concentrations in Phantoms Without Coffee

| Percentage Absolute Error (%)                 | Error   | Estimated Concentration (mg/dL) | Actual Concentration (mg/dL) | Reflected Light Intensity (a.u.) |      |     |
|---|---------|---------------------------------|------------------------------|----------------------------------|------|-----|
|   |         |                                 |                              | Green                            | Blue | Red |
| -3.8400                                       | -0.0096 | 0.2404                          | 0.25                         | 682                              | 435  | 408 |
| 25.1667                                       | 0.0755  | 0.3755                          | 0.30                         | 680                              | 400  | 396 |
| 1.7000  | 0.0085  | 0.5085                          | 0.50                         | 699                              | 380  | 399 |
| -3.9350                                       | -0.0787 | 1.9213                          | 2                            | 709                              | 170  | 380 |
| -6.0000                                       | -0.1800 | 2.8200                          | 3                            | 700                              | 101  | 398 |
| -4.1500                                       | -0.1660 | 3.8340                          | 4                            | 500                              | 42   | 390 |
| Pearson Correlation Coefficient: $r = 0.9997$ |         |                                 |                              |                                  |      |     |

Table 2 Reflected Light Intensity at Different Bilirubin Concentrations in Coffee-Infused Phantoms

| Percentage Absolute Error (%)                 | Error   | Estimated Concentration (mg/dL) | Actual Concentration (mg/dL) | Reflected Light Intensity (a.u.) |      |     |
|---|---------|---------------------------------|------------------------------|----------------------------------|------|-----|
|   |         |                                 |                              | Green                            | Blue | Red |
| -2.2000                                       | -0.0055 | 0.2445                          | 0.25                         | 341                              | 217  | 204 |
| 25.1667                                       | 0.0755  | 0.3755                          | 0.30                         | 340                              | 200  | 198 |
| 27.8200                                       | 0.1391  | 0.6391                          | 0.50                         | 390                              | 190  | 170 |
| -3.8250                                       | -0.0765 | 1.9235                          | 2                            | 355                              | 85   | 190 |
| -6.3767                                       | -0.1913 | 2.8087                          | 3                            | 404                              | 56   | 160 |
| 1.3825  | 0.0553  | 4.0553                          | 4                            | 388                              | 27   | 188 |
| Pearson Correlation Coefficient: $r = 0.9976$ |         |                                 |                              |                                  |      |     |

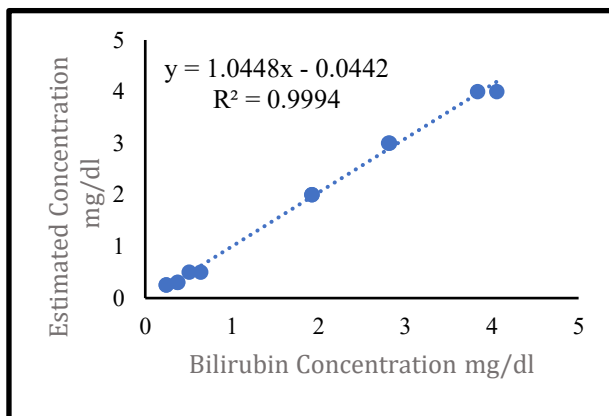


Fig. 7 Estimated Bilirubin Concentrations at Different Actual Levels in Phantoms Without Coffee

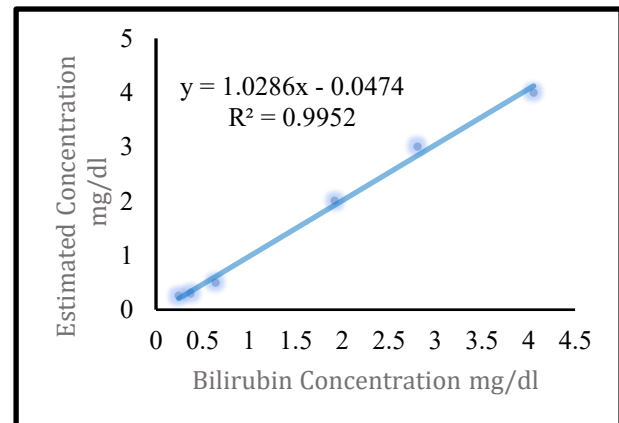


Fig. 8 – Estimated Bilirubin Concentrations at Different Actual Levels in Coffee-Infused Phantoms

In addition to the correlation coefficient, analysis of percentage error is crucial for assessing measurement accuracy. In this study, the percentage error ranged from 1.3825% to 27.8200%. The highest error was observed at a bilirubin concentration of 0.5 mg/dL, while the lowest error occurred at 4 mg/dL.

This variation in error percentage may result from several factors, including the limited sensitivity of the device at lower concentrations, human errors during measurement, or slight variations in experimental and environmental conditions.

#### IV. ANALYSIS OF EXPERIMENTAL RESULTS

The present study was conducted to evaluate the accuracy and effectiveness of a non-invasive method for measuring bilirubin concentration in neonates. To assess the validity and positioning of the proposed approach, the results were compared with those reported in previous studies.

In the study by Surana et al., a Pearson correlation coefficient of 0.69 was reported between the invasive (blood test) and non-invasive (JM-103 device) methods [14], indicating a moderate correlation. Other studies reported correlation values of 0.9997, 0.88, and



0.953, respectively [11–13]. In contrast, the device developed in this study demonstrated a correlation coefficient of over 0.9976, despite its low cost (under 5 million IRR), highlighting its high potential for screening applications.

Measurements were performed based on optical principles using wavelengths directly related to bilirubin absorption. One of the key advantages of the device is its resilience to environmental interferences, such as ambient light and temperature changes. Additionally, through precise calibration and intelligent algorithms, it minimizes the effects of physical variables such as skin thickness and surface moisture.

Another notable strength is the system's ability to compensate for different skin tones. Since melanin can significantly affect light reflection and absorption, the device design incorporates multi-band optical filters and dynamic calibration to adapt to various pigmentation levels. Experimental results confirmed consistent accuracy across light, medium, and dark skin tones.

This feature is particularly important in multi-ethnic clinical environments, where measurement reliability across all patients is crucial. The higher correlation coefficients observed in this study compared to previous works reflect the superior accuracy of the proposed method. This may be attributed to several factors, including advanced hardware design, use of high-sensitivity sensors, complex signal processing algorithms, and robust calibration techniques. Additionally, differences in sample type (phantoms vs. human subjects) may partially explain the variability observed across studies. Although the gelatin-based phantoms closely mimic the optical properties of human skin, their surface is smoother than natural skin. In this study, a thin matte coating was applied to promote uniform light diffusion and minimize the impact of surface smoothness. Additionally, maintaining a fixed distance between the sensor and the sample further reduced surface-related variability.

## V. CONCLUSION

This study focused on the design and development of a portable photometric device for the non-invasive measurement of transcutaneous bilirubin levels in neonates. Leveraging advanced optical technologies and digital signal processing, the device demonstrated high accuracy and minimal error, even in the presence of environmental interferences and individual variations such as skin pigmentation.

The integration of stable light sources, precise optical filters, and an intelligent calibration system enabled reliable and repeatable results. Furthermore, the use of gelatin-based phantoms with standardized chromophores provided a suitable model for simulating human skin and assessing the device's performance under controlled laboratory conditions.

With its compact size and low weight, the device offers excellent portability and can serve as an effective tool for early jaundice detection, particularly in clinical and underserved settings. Key advantages include non-invasiveness, rapid measurement, reduced infection risk, and ease of use.

Given the critical importance of timely diagnosis and treatment of neonatal jaundice in preventing serious complications, further development of similar devices with advanced features—such as integration with intelligent systems and real-time data analysis—is highly recommended.

It is worth noting that the device is currently undergoing clinical evaluation, with initial human testing being conducted at a medical facility affiliated with Jahrom University of Medical Sciences, under approved ethical protocols.

## REFERENCES

- [1] M. Penhaker, V. Kasik, and B. Hrvolová, "Advanced bilirubin measurement by a photometric method," *Elektronika ir Elektrotechnika*, vol. 19, no. 3, pp. 47–50, 2013.

- [2] T. Mulquiney and S. Dechert, "Health problems of the newborn," in *Wong's Nursing Care of Infants and Children*, Australia and New Zealand Edition, E-book for Professionals, 2021, p. 168.
- [3] E. I. Obeagu and M. C. Katya, "A systematic review on physiological jaundice: Diagnosis and management of the affected neonates," *Madonna Univ. J. Med. Health Sci.*, vol. 2, no. 3, pp. 25–41, 2022.
- [4] C. I. Okwundu et al., "Transcutaneous bilirubinometry versus total serum bilirubin measurement for newborns," *Cochrane Database Syst. Rev.*, no. 5, 2023.
- [5] F. A. Dzulkifli, M. Y. Mashor, and K. Khalid, "Methods for determining bilirubin level in neonatal jaundice screening and monitoring: A literature review," *J. Eng. Res. Educ.*, vol. 10, pp. 1–10, 2018.
- [6] C. J. Hazarika et al., "Development of non-invasive biosensors for neonatal jaundice detection: A review," *Biosensors*, vol. 14, no. 5, p. 254, 2024.
- [7] J. Chahl, "Non-invasive and non-contact automatic jaundice detection of infants based on random forest," *Comput. Methods Biomech. Biomed. Eng. Imaging Vis.*, vol. 11, pp. 2516–2529, 2023.
- [8] L. Zucchini et al., "Optimization of an algorithm for hemoglobin interference compensation on a simple photometer for bilirubin measurement," in *Proc. IEEE Int. Symp. Med. Meas. Appl. (MeMeA)*, Eindhoven, Netherlands, 2024, pp. 1–6.
- [9] M. Johnson, *Photodetection and Measurement: Maximizing Performance in Optical Systems*. New York, NY, USA: McGraw-Hill, 2003.
- [10] N. Bint Ali, "ANN-based non-invasive jaundice measurement system using optical technique," M.S. thesis, Univ. Tun Hussein Onn, Malaysia, 2023.
- [11] N. Y. Cheng, Y. L. Lin, M. C. Fang, W. H. Lu, C. C. Yang, and S. H. Tseng, "Noninvasive transcutaneous bilirubin assessment of neonates with hyperbilirubinemia using a photon diffusion theory-based method," *Biomed. Opt. Express*, vol. 10, pp. 2969–2984, 2019.
- [12] Y. Y. Chen, S. Y. Tzeng, Y. L. Lin, K. Y. Chu, and S. H. Tseng, "Precisely discerning the bilirubin concentration of turbid samples using diffuse reflectance spectroscopy," *Front. Opt.*, 2016.
- [13] N. Y. Cheng, S. Y. Tzeng, M. C. Fang, C. Y. Kuo, W. H. Lu, C. C. Yang, and S. H. Tseng, "Handheld diffuse reflectance spectroscopy system for noninvasive quantification of neonatal bilirubin and hemoglobin concentrations: A pilot study," *Biomed. Opt. Express*, vol. 14, pp. 467–476, 2023.
- [14] A. U. Surana et al., "Comparison of transcutaneous bilirubin with serum bilirubin measurements in neonates at tertiary care center in western part of India," *Int. J. Contemp. Pediatr.*, vol. 4, no. 4, pp. 1445–1449, 2017.
- [15] J. H. Chou, "Predictive models for neonatal follow-up serum bilirubin: Model development and validation," *JMIR Med. Inform.*, vol. 8, no. 10, 2020.
- [16] G. Koch et al., "Leveraging predictive pharmacometrics-based algorithms to enhance perinatal care—Application to neonatal jaundice," *Front. Pharmacol.*, vol. 13, p. 842548, 2022.
- [17] L. Zucchini et al., "A method for compensating hemoglobin interference in total serum bilirubin measurement using a simple two-wavelength reflectance photometer," *Sensors*, vol. 24, no. 20, p. 6749, 2024.
- [18] M. Thomas et al., "Current and emerging technologies for the timely screening and diagnosis of neonatal jaundice," *Crit. Rev. Clin. Lab. Sci.*, vol. 59, no. 5, pp. 332–352, 2022.
- [19] D. F. Swinehart, "The Beer–Lambert law," *J. Chem. Educ.*, vol. 39, no. 7, p. 333, 1962.